Pan *et al. Geotherm Energy* (2020) 8:6
https://doi.org/10.1186/s40517-020-0161-4

Geothermal Energy

RESEARCH

Open Access

Optimization of the utilization of deep borehole heat exchangers

Sheng Pan[1,2,3], Yanlong Kong[1,2,3*], Chaofan Chen[4], Zhonghe Pang[1,2,3] and Jiyang Wang[1,2,3]

*Correspondence:
ylkong@mail.iggcas.ac.cn
[1] Key Laboratory of Shale Gas and Geoengineering, Institute of Geology and Geophysics, Chinese Academy of Sciences, Beijing 100029, China
Full list of author information is available at the end of the article

Abstract

Deep-borehole heat exchangers (DBHE) are generally coaxial pipes installed in deep boreholes and has become an alternative approach to utilize geothermal energy. Since the performance of the DBHE system can be affected by several parameters, it is important to optimize the design of parameters for the DBHE. In this paper, based on the analytical method, we carried out the sensitivity analysis of DBHE design parameters, including outer pipe diameter, inner pipe diameter, flow rate, outer pipe materials, grout materials, and borehole depth during continuous operation for 4 months. The sensitivity analysis results indicate that the heat extraction rate can be significantly affected by outer pipe diameter, borehole depth, and flow rate. The effects of grout materials, inner pipe diameter and outer pipe materials are of second-order. Finally, an optimization method based on the lowest Average Energy Cost index was proposed to optimize these DBHE design parameters under different geological conditions. Given the cost in this study, a combination scheme of all the optimal parameters is given for different depth wells under different geological conditions.

Keywords: Deep-borehole heat exchanger, Geothermal energy, Sensitivity analysis, Optimal heat extraction rate, Economic analysis

Introduction

Based on the differences in burial depth, utilization mode, and storage medium, geothermal energy is usually divided into three types: shallow geothermal energy (0–200 m), medium–deep hydrothermal energy (200–3000 m), and hot dry rocks energy (> 3000 m) (Wang 2015). The China Geothermal Energy Development Report released in August 2018 shows that the shallow geothermal energy is the main method used in China for geothermal heating, which has been rapidly developed. The extent of hydrothermal heating is also increasing steadily. However, the development in the utilization of geothermal resources has some difficulties due to the large areas demanding of shallow geothermal energy and the uneven distribution of hydrothermal energy (Kong et al. 2014). Moreover, when utilizing the hydrothermal energy, reinjection of geothermal wastewater must be carried out for maintaining the pressure of geothermal reservoirs (Rybach 2003). However, with a low reinjection rate, reinjection could be quite difficult in sandstone reservoirs (Kong et al. 2014; Su et al. 2018; Ungemach 2003). Therefore, deep-borehole heat exchangers (DBHE) have become an alternative approach to utilize geothermal energy (Alimonti et al. 2018). The principle of DBHE is to install a coaxial pipe into a deep borehole to inject cold water into the outer pipe and extract hot water from the inner pipe, forming a closed-loop system (Rybach and Hopkirk 1995). The heat energy can be transported during this process through the heat transfer between circulating fluid and surrounding rock. There is no interaction between circulating fluid and natural groundwater; it is thus called "obtaining heat without extracting groundwater".

It could be found that the principle of DBHE is quite similar to the coaxial borehole heat exchangers (CBHE) except for the depth (Acuña et al. 2011; Holmberg et al. 2016; Kohl et al. 2002; Sapinska-Sliwa et al. 2016). However, at least to the authors' knowledge, the definition of DBHE depth range does not appear in any literature. In this study, the borehole heat exchangers (BHE) deeper than 500 m were defined as DBHE in consideration of the heat exchanging efficiency. The research on BHE carried out in the last decade concerns detailed investigations of the heat transfer performance of CBHE and DBHE.

For the CBHE, several studies have focused on investigating its performance and applicability. Acuña et al. (2011) implemented six distributed thermal response tests (DTRTs) on a multi-pipe CBHE. Acuña and Palm (2013) presented results from three DTRTs carried out on two coaxial pipe-in-pipe BHE at different flow rates. They pointed out that the ground thermal conductivity and the borehole thermal resistance required for designing a CBHE system could be determined by an in situ thermal response test on a completed borehole. Zanchini et al. (2010) investigated the effects of thermal short-circuiting and flow velocity on the thermal efficiency of CBHE. The results show that the effects of flow velocity and thermal short-circuiting are both important and that the latter can be reduced considerably by employing a low conductivity material for the inner tube. Raymond et al. (2015) evaluated the impact of changing the water flow rate, the inner and outer pipe SDR on the thermal resistance of CBHE. The results show that considerable advantages could be obtained by increasing the water flow rate, and the outer pipe SDR. Beier et al. (2013) developed a CBHE model for the vertical temperature profiles, which can be used instead of the mean temperature approximation to estimate borehole resistance. Furthermore, Luo et al. (2019) presented an analytical model for CBHE that specifically considers geothermal gradient.

Over the past few years, more and more research work has been carried out to investigate the DBHE system performance. Several studies suggest that the heat transfer performance of the DBHE correlates significantly with the geothermal gradient and thermal conductivity of the surrounding rock (Bu et al. 2012; Chen et al. 2019; Cheng et al. 2013; Kong et al. 2017a, b; Le Lous et al. 2015; Nalla et al. 2005; Noorollahi et al. 2015; Templeton et al. 2014). Le Lous et al. (2015) also conducted the sensitivity analysis of the volumetric heat capacity of the rock. They found that low volumetric heat capacity value can reduce the thermal recovery time. Except for geological conditions, parameters related to DBHE design and operational settings can also affect the heat performance of DBHE. Fang et al. (2018), Holmberg et al. (2016), and Wang et al. (2017) found that the circulating fluid injected through the annular space can reduce the heat loss than through the inner pipe. Moreover, the performance of different circulating fluids in such heat transfer has been evaluated, proving that water is the most suitable fluid for circulation

(Alimonti and Soldo 2016; Bu et al. 2012; Kujawa et al. 2004; Le Lous et al. 2015; Nalla et al. 2005; Noorollahi et al. 2015; Templeton et al. 2014; Wight and Bennett 2015).

Furthermore, Nalla et al. (2005) pointed out that a key parameter affecting the performance of the DBHE is the fluid residence time, which represents the flow rate. The other DBHE design parameters have also been investigated, including the borehole diameter, the diameter of the outer pipe, the diameter of the inner pipe, the depth of the borehole, grout materials and pipe materials (Alimonti and Soldo 2016; Beier and Holloway 2015; Chen et al. 2019; Lhendup et al. 2014; Nalla et al. 2005; Wang et al. 2017). According to the results of these analyses, borehole diameter, the outer pipe diameter, grout thermal conductivity, outer pipe thermal conductivity, and borehole depth can positively influence the heat transfer performance of DBHE (Alimonti and Soldo 2016; Chen et al. 2019; Nalla et al. 2005; Wang et al. 2017). In contrast, the inner pipe diameter and inner pipe wall thermal conductivity could negatively influence the heat transfer performance of DBHE (Alimonti and Soldo 2016; Beier and Holloway 2015; Chen et al. 2019; Lhendup et al. 2014; Nalla et al. 2005). Therefore, it can be concluded that all these DBHE design parameters can affect the system performance, and the optimal design of DBHE can be obtained, while it was rarely given in the literature.

Herein, we simulated the effects of design parameters such as outer and inner pipe diameter, flow rate, grout and outer pipe materials, and DBHE depth on the heat extraction rate. The parametric sensitive study is conducted by using the analytical method proposed by Beier (2014) and Beier et al. (2014). Importantly, our study revealed that it is useful for improving the DBHE system performance to allocate these design parameters simultaneously. Further, we developed an optimization method to identify the optimal DBHE configuration in different regions. We considered 3 rock types of sandstone, limestone, and granite due to their wide distribution and utilization for geothermal energy exploitation. Since the optimal design for the DBHE is to improve the heat transfer capacity and reduce the cost, our optimization method is to do the economic analysis by applying the Average Energy Cost (AEC) index (Rodríguez and Díaz 2009).

Methods

Optimization method

In this study, we used the index of Average Energy Cost to optimize the DBHE design, which includes the outer pipe diameter, inner pipe diameter, flow rate, outer pipe materials, grout materials, and DBHE depth.

The average energy cost represents the specific cost of heat in yuan per kilowatt-hour. It was calculated from the total well cost, which consists of the drilling cost C_{drill}, grout cost C_{grout}, coaxial pipe cost C_{pipe}, and circulating water cost C_{water}, and is divided by the system's thermal energy output Q:

$$AEC = \frac{C_{\text{drill}} + C_{\text{grout}} + C_{\text{pipe}} + C_{\text{water}}}{Q}. \quad (1)$$

The system's thermal energy output Q is calculated with heat extraction rate, DBHE depth, and working time. In this study, we defined the heat extraction rate as the maximum rate at which the inlet temperature is near to 0 °C at the end of a heat extraction period. Fang et al. (2018) used a similar definition for the optimal rate of heat extraction, where inlet temperature is maintained at 5 °C at the end of a period of heat extraction. In addition, the analytical method used for calculating the heat extraction rate is given in "Coaxial heat exchanger model" section.

The drilling cost for different borehole diameter intervals is presented in Budget Standard of Geological Survey Projects by China Geological Survey (https://max.book118.com/html/2017/0903/131520083.shtm), but only 4 ranges (#1–4) of borehole diameter are given, and the depth range is 500–1000 m. In order to calculate the AEC of DBHE with a depth range of 500–3000 m, the drilling cost of other depth is calculated by the relation between well depth and drilling cost (Daniilidis et al. 2017; Heidinger 2010; Olasolo et al. 2016), as shown in Table 1. The borehole diameter intervals of #1–4 are 201–250 mm, 251–300 mm, 301–350 mm, 351–400 mm, respectively. It is, therefore, with a constant thickness of grout between the outer pipe and the surrounding soil (0.023 m), the outer pipe diameter intervals of #1–4 are 0.178–0.227 m, 0.228–0.277 m, 0.278–0.327 m, 0.328–0.377 m, respectively. The coaxial pipe cost is calculated based on the weight per length of coaxial pipe, and a fixed cost per unit mass of steel (Nalla et al. 2005). The normalized coaxial loop cost is 7 yuan per linear foot of loop, which consists of a 1-in. inner pipe and a 4-in. outer pipe (Liu et al. 2018). The circulating water cost is calculated based on the volume of water, and the normalized water cost is 0.0021 yuan per gallon (Liu et al. 2018). The grout cost is calculated based on the volume of grout used for sealing the outer pipe diameter. The normalized grout cost is 2.310 yuan per gallon (Liu et al. 2018), and the thermally enhanced grout is 7 and 10.5 yuan per gallon (Liu et al. 2018).

The principle of the optimization is to find the DBHE design with minimum AEC value. Since the AEC is highly related to the heat transfer performance of DBHE, the key to minimize the AEC of DBHE is to obtain the optimal heat transfer efficiency. The optimization procedures are as illustrated in Fig. 1, and the details are as follows.

Table 1 The drilling cost of different borehole diameter intervals and rock types

Rock type	#1 (yuan/m)	#2 (yuan/m)	#3 (yuan/m)	#4 (yuan/m)	BHE depth (m)
Sandstone	1497	1599	2135	2393	500
Sandstone	2994	3198	4270	4786	1000
Sandstone	5988	6396	8540	9572	1500
Sandstone	8982	9594	12,810	14,358	2000
Sandstone	11,976	12,792	17,080	19,144	2500
Sandstone	17,964	19,188	25,620	28,716	3000
Limestone	2159	2374	3086	3450	500
Limestone	4318	4748	6172	6900	1000
Limestone	8636	9496	12,344	13,800	1500
Limestone	12,954	14,244	18,516	20,700	2000
Limestone	17,272	18,992	24,688	27,600	2500
Limestone	25,908	28,488	37,032	41,400	3000
Granite	3670	4036	5246	5865	500
Granite	7340	8072	10,492	11,730	1000
Granite	14,680	16,144	20,984	23,460	1500
Granite	22,020	24,216	31,476	35,190	2000
Granite	29,360	32,288	41,968	46,920	2500
Granite	44,040	48,432	62,952	70,380	3000

The first step is to choose the simulated scenario of certain DBHE materials, DBHE depth, and rock type. The second step is varying the outer pipe diameter and choosing one. The third step is to obtain the inner pipe diameter by matching the annular space area with the area of the cross-section of the inner pipe. The fourth step is to modify the flow rate to obtain the relationship between the flow rate and heat extraction rate. The fifth step is calculating the approximate gradient of each flow rate and select the optimal flow rate where the gradient decreases to a minimum (in our study, this was when the gradient was less than 0.2/0.5 = 0.4). The sixth step is to calculate the optimal heat extraction rate with the obtained pipes diameter and flow rate. The seventh step is calculating the AEC value of this DBHE design. The eighth step is calculating the AEC values of other DBHE designs by redoing step 2 to step 7. Finally, the ninth step is finding the optimal DBHE design with the lowest AEC values.

Coaxial heat exchanger model

In this study, we applied the analytical method proposed by Beier (2014) and Beier et al. (2014) to calculate the heat extraction rate. In their method, the governing equations of heat transfer in the inner pipe, outer pipe, grout, and ground are established, respectively. The two equations in pipes are coupled together by the shunt heat transfer through the wall of the inner pipe. The fluid flowing through the annulus exchanges heat with the surrounding

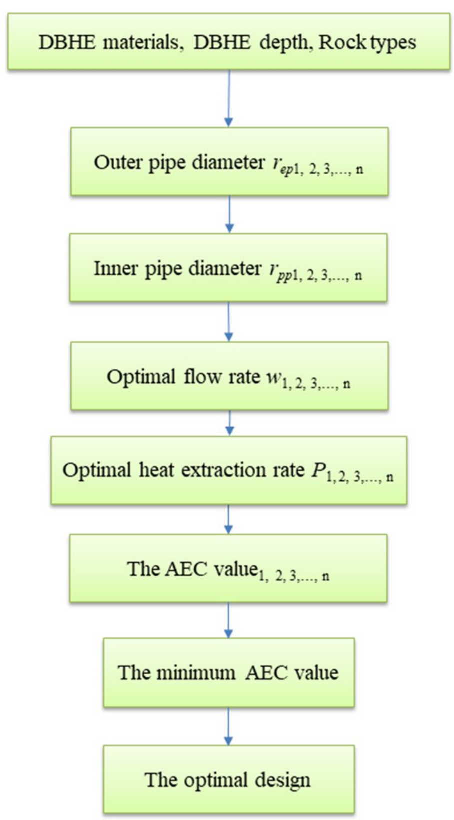

Fig. 1 Procedure to obtain the optimal design of DBHE with a total of n scenarios

grout. Heat conduction through the grout and ground occurs radially out from the outer pipe. The circulating fluid enters the BHE through the annulus in this model.

The energy conservation equation of the annulus is

$$\frac{\partial T_{D1}}{\partial z_D} + \frac{N_s H_f A_{D1}}{2}\frac{\partial T_{D1}}{\partial t_D} + N_{12}(T_{D1} - T_{D2}) + N_g\left(T_{D1} - T_{Dg}\right)_{r_D=1} = 0, \quad (2)$$

$$0 < Z_D < 1, \quad 0 < t_D$$

where N_s is a dimensionless thermal conductance (reciprocal of resistance) of the ground, the symbol w represents the flow rate, and N_g is a dimensionless thermal conductance (reciprocal of resistance) of the grout. The ratio of the volumetric heat capacities of the circulating fluid, c_f, and the ground, c_s, is designated as H_f. The parameter A_{D1} is a ratio of the flow area.

The energy conservation equation of the inner pipe is

$$-\frac{\partial T_{D2}}{\partial z_D} + \frac{N_s H_f A_{D2}}{2}\frac{\partial T_{D1}}{\partial t_D} + N_{12}(T_{D2} - T_{D1}) = 0, \quad 0 < Z_D < 1, 0 < t_D. \quad (3)$$

The parameter A_{D2} is a ratio of the inner pipe area and the circular area based on the outside pipe outer wall radius.

Neglecting heat conduction in the axial direction, the heat conduction equation for the grout is

$$\frac{H_g}{\kappa}\frac{\partial T_{Dg}}{\partial t_D} = \frac{1}{r_D}\frac{\partial T_{Dg}}{\partial r_D} + \frac{\partial T_{Dg}^2}{\partial r_D^2}, \quad 1 < r_D < r_{Db}, 0 < z_D < 1, 0 < t_D. \quad (4)$$

The heat conduction equation for the ground surrounding the borehole is

$$\frac{\partial T_{Ds}}{\partial t_D} = \frac{1}{r_D}\frac{\partial T_{Ds}}{\partial r_D} + \frac{\partial T_{Ds}^2}{\partial r_D^2}, \quad r_{Db} < r_D, 0 < z_D < 1, 0 < t_D. \quad (5)$$

Equations (1) and (2) require boundary conditions. When $z_D = 0$, there is

$$(T_{D1} - T_{D2}) = N_s,\ z_D = 0, \quad 0 < t_D. \quad (6)$$

When $z_D = 1$, there is,

$$T_{D1} = T_{D2},\ z_D = 1, \quad 0 < t_D. \quad (7)$$

At the outer pipe/grout interface where r_D=1, an energy balance sets the heat transfer from the circulating fluid to the grout equal to the heat conducted into the grout. That is,

$$\frac{N_g\left(T_{Dg} - T_{D1}\right)}{\kappa N_s} = \frac{\partial T_{Dg}}{\partial r_D}, \quad r_D = 1, 0 < z_D < 1, 0 < t_D. \quad (8)$$

At the grout/ground interface, $r_D = r_{Db}$, an energy balance sets the heat conduction rate from the grout equal to the heat conduction rate into the ground, and the grout and ground temperatures are equal at this interface,

$$\kappa\frac{\partial T_{Dg}}{\partial r_D}=\frac{\partial T_{Ds}}{\partial r_D},\ r_D=r_{Db},\quad 0<z_D<1,0<t_D, \tag{9}$$

$$\partial T_{Dg}=\partial T_{Ds},\ r_D=r_{Db},\quad 0<z_D<1,\ 0<t_D. \tag{10}$$

The ground temperature approaches its undisturbed value as the distance from the borehole increases,

$$\partial T_{Ds}\to 0, as r_D\to\infty,\quad 0<z_D<1,0<t_D. \tag{11}$$

At the start of heat injection ($t_D = 0$), the circulating fluid, grout, and ground are all at the undisturbed ground temperature. This condition requires the dimensionless temperatures to be zero,

$$T_{D1}=T_{D2}=0,\quad 0\le z_D\le 1,\quad t_D=0, \tag{12}$$

$$T_{\mathrm{Dg}}=0,\quad 1\le r_D\le r_{Db},\quad 0\le z_D\le 1,\quad t_D=0, \tag{13}$$

$$T_{Ds}=0,\quad r_{Db}\le r_D,\quad 0\le z_D\le 1,\quad t_D=0. \tag{14}$$

Detailed calculation of the heat transfer coefficient and the analytical solution can be found in references of Beier et al. (2014).

Sensitivity analysis and simulated scenarios

The principle of the sensitivity analysis is that when analyzing the impact of one parameter on the heat extraction rate of DBHE, the other parameters should be kept fixed. In this study, we performed the sensitivity analysis of each design parameter (outer pipe diameter, inner pipe diameter, flow rate, outer pipe materials, grout materials, and depth) by applying the coaxial pipe heat exchanger model. The parameters in the model are given in Table 2, and the system running time is a heating cycle of 4 months.

Besides, in order to investigate the applicability of DBHE in different rock types, 3 rock types (sandstone, limestone, granite) were chosen in the calculation. Furthermore, we considered the average, minimum, and maximum values of thermal conductivity for the selected rock types. Since the heat capacity of selected rock types changes little under constant temperature, we chose the mean value of rock volumetric heat capacity (Clauser 2011a, b; McKenna et al. 1996; Thomas et al. 1973; Cho et al. 2009). Table 3 summarizes the details of the thermal properties of selected rock types. With these considerations, we established 54 scenarios to simulate the effect of each design parameter. The overview of these scenarios is listed in Table 4, and the details of each scenario are as follows.

In order to analyze the effects of outer pipe diameter on the heat extraction rate, the diameter was set at 0.177, 0.180 m, and then increased incrementally in 0.020 m steps, while keeping all other parameters that act upon the DBHE constant. This was repeated until the outer pipe reached a diameter of 0.400 m. Using this method, the diameter of the borehole increases accordingly. Besides, we set the thickness of the grout between the outer pipe and the surrounding soil at 0.023 m. Recognizing that the heterogeneity of geological materials strongly affects the heat transfer

Table 2 Parameters used in the model

Parameter	Symbol	Amount	Unit
Borehole diameter	d_b	0.2	m
Inner pipe outer diameter	d_{po}	0.09	m
Inner pipe wall thickness	t_i	0.00734	m
Outer pipe outer diameter	d_{eo}	0.177	m
Outer pipe wall thickness	t_e	0.00587	m
Flow rate	w	11.6	L s^{-1}
Pipe wall thermal conductivity	k_{pp}, k_{ep}	0.5	W m^{-1} K^{-1}
Grout thermal conductivity	k_g	0.73	W m^{-1} K^{-1}
Grout volumetric heat capacity	c_g	3.8×10^6	J m^{-3} K^{-1}
Water density	ρ	1000	kg m^{-3}
Water volumetric heat capacity	c_f	4.19×10^6	J m^{-3} K^{-1}
Water thermal conductivity	k_f	0.59	W m^{-1} K^{-1}
Water viscosity	μ_f	1.14×10^{-3}	kg m^{-1} s^{-1}
Water Prandtl number	Pr	8.09	–
Average ground temperature	T_s	15	°C
Borehole depth	D	2000	m

Table 3 Values of thermal properties for the selected rock types

Rock type	Minimum thermal conductivity value (W m^{-1} K^{-1})	Average thermal conductivity value (W m^{-1} K^{-1})	Maximum thermal conductivity value (W m^{-1} K^{-1})	Volumetric heat capacity (J m^{-3} K^{-1})
Sandstone	2.06	3.895	5.73	2.05×10^6
Limestone	1.2	2.15	3.1	2.155×10^6
Granite	2.12	2.87	3.62	2.33×10^6

performance of DBHE, the influence of outer pipe diameter on the heat extraction rate was carried out under different geological conditions (scenario #1A–I).

In order to investigate the influences of the inner pipe diameter, the parameters in the DBHE were kept constant except the change of inner pipe diameter. Since the diameter of the inner pipe cannot exceed that of the outer pipe, the range of inner pipe diameters is 0.050–0.140 m and the increment used for analysis is 0.010 m, totaling 10 steps. Since rocks are heterogeneous materials, the impact of inner pipe diameter on heat extraction rate was investigated under different geological conditions (scenario #2A–I).

For the analysis of the effects of flow rate on heat extraction rate, other parameters in the DBHE were maintained at a constant level, and the flow rate was changed. The range of the calculated flow rate is 11.6–81.6 L s^{-1}, with an incremental step of 5.0 L s^{-1} used for the analysis. The range of Reynolds number of the inner pipe is from 172,010 to 1,210,000, and the range of Reynolds number of the outer pipe is from 50,755 to 357,040. Scenarios #3A–I were designed to investigate the impact of flow rate on heat extraction rate under different geological conditions.

For the analysis of the change in heat extraction rate with different outer pipe materials, we considered three outer pipe wall thermal conductivity values (0.5, 30, 45) in the calculation. The first one represents the concrete outer pipe, and the last two

Table 4 Simulated scenarios for the sensitivity analysis

Scenario ID	Outer pipe diameter (m)	Inner pipe diameter (m)	Flow rate (L s^{-1})	Outer pipe wall thermal conductivity (W m^{-1} K^{-1})	Grout thermal conductivity (W m^{-1} K^{-1})	DBHE depth (m)	Rock type	Description
#1A-C	Var	0.09	11.6	0.5	0.73	2000	Sandstone	#1A, #1D, #1G correspond to the minimum thermal conductivity value
#1D-F	Var	0.09	11.6	0.5	0.73	2000	Limestone	#1B, #1E, #1H correspond to the average thermal conductivity value
#1G-I	Var	0.09	11.6	0.5	0.73	2000	Granite	#1C, #1F, #1I correspond to the maximum thermal conductivity value
#2A-C	0.177	Var	11.6	0.5	0.73	2000	Sandstone	#2A, #2D, #2G correspond to the minimum thermal conductivity value
#2D-F	0.177	Var	11.6	0.5	0.73	2000	Limestone	#2B, #2E, #2H correspond to the average thermal conductivity value
#2G-I	0.177	Var	11.6	0.5	0.73	2000	Granite	#2C, #2F, #2I correspond to the maximum thermal conductivity value
#3A-C	0.177	0.09	Var	0.5	0.73	2000	Sandstone	#3A, #3D, #3G correspond to the minimum thermal conductivity value
#3D-F	0.177	0.09	Var	0.5	0.73	2000	Limestone	#3B, #3E, #3H correspond to the average thermal conductivity value

Table 4 (continued)

Scenario ID	Outer pipe diameter (m)	Inner pipe diameter (m)	Flow rate (L s^{-1})	Outer pipe wall thermal conductivity (W m^{-1} K^{-1})	Grout thermal conductivity (W m^{-1} K^{-1})	DBHE depth (m)	Rock type	Description
#3G-I	0.177	0.09	Var	0.5	0.73	2000	Granite	#3C, #3F, #3I correspond to the maximum thermal conductivity value
#4A-C	0.177	0.09	11.6	Var	0.73	2000	Sandstone	#4A, #4D, #4G correspond to the minimum thermal conductivity value
#4D-F	0.177	0.09	11.6	Var	0.73	2000	Limestone	#4B, #4E, #4H correspond to the average thermal conductivity value
#4G-I	0.177	0.09	11.6	Var	0.73	2000	Granite	#4C, #4F, #4I correspond to the maximum thermal conductivity value
#5A-C	0.177	0.09	11.6	0.5	Var	2000	Sandstone	#5A, #5D, #5G correspond to the minimum thermal conductivity value
#5D-F	0.177	0.09	11.6	0.5	Var	2000	Limestone	#5B, #5E, #5H correspond to the average thermal conductivity value
#5G-I	0.177	0.09	11.6	0.5	Var	2000	Granite	#5C, #5F, #5I correspond to the maximum thermal conductivity value
#6A-C	0.177	0.09	11.6	0.5	0.73	var	Sandstone	#6A, #6D, #6G correspond to the minimum thermal conductivity value

Table 4 (continued)

Scenario ID	Outer pipe diameter (m)	Inner pipe diameter (m)	Flow rate (L s^{-1})	Outer pipe wall thermal conductivity (W m^{-1} K^{-1})	Grout thermal conductivity (W m^{-1} K^{-1})	DBHE depth (m)	Rock type	Description
#6D-F	0.177	0.09	11.6	0.5	0.73	var	Limestone	#6B, #6E, #6H correspond to the average thermal conductivity value
#6G-I	0.177	0.09	11.6	0.5	0.73	var	Granite	#6C, #6F, #6I correspond to the maximum thermal conductivity value

represents pipes made of steel. Further, nine scenarios (#4A–I) were designed to investigate the impact of outer pipe wall thermal conductivity on the heat extraction rate under different geological conditions.

Subsequently, we applied three types of grout materials in the simulation to analyze the influences of grout materials. The first one is bentonite–water mixtures with thermal conductivity value of 0.73, the second one is a mix of bentonite and silica sand with thermal conductivity value of 1.73, and the last one is a mix of bentonite and graphite with thermal conductivity value of 2.77 (Liu et al. 2018). Furthermore, we designed nine scenarios (#5A-F) to investigate the impact of outer pipe wall thermal conductivity on the heat extraction rate under different geological conditions.

We also changed the DBHE depths to see what effect they had on heat transfer capacity. In our study, the depth range was set from 500 to 3000 m, with an incremental step of 500 m. Then, scenarios #6A–I were designed to investigate the influences of DBHE depth on the heat extraction rate under different geological conditions.

Results and discussion

The sensitivity analysis of DBHE design parameters

The influence of outer pipe diameter

In scenario #1A–I, the simulated results of the heat extraction rate with different outer pipe diameter under different geological conditions are presented in Fig. 2. Figure 2 suggests that as the diameter of the outer pipe increases, the associated increase in heat extraction rate gradually decreases. The heat extraction rate is more sensitive to the increase of the outer pipe diameter when the pipe is smaller and does not linearly increase with outer pipe diameter. For example, in scenario #1B, when we increase the diameter from 0.180 to 0.220 m, the heat extraction rate increases from 178 to 190 W m^{-1} (increase by 6.7%). However, when the outer pipe diameter increases from 0.360 m to 0.400 m, the heat extraction rate only increases from 221.7 to 229.1 W m^{-1} (increase by 3.3%). The heat extraction rate is, therefore, more sensitive to increases in the outer pipe diameter while the pipe remains relatively small. Wang et al. (2017) also

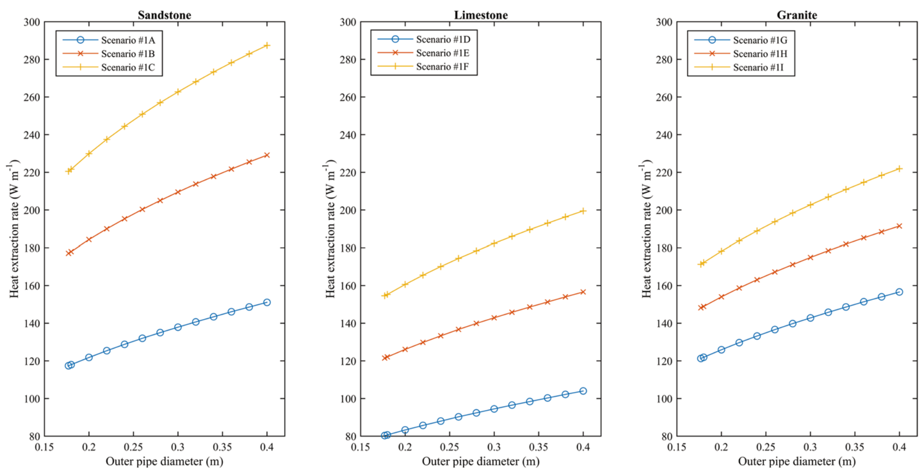

Fig. 2 Influence of different outer pipe diameter on heat extraction rate under different geological conditions

simulated the outlet temperature and heat transfer capacity under different outer pipe diameters. The results demonstrate that the outlet temperature and heat transfer capacity both increase with an increase to the outer pipe diameter. Because this study is concerned with changes in the optimal heat extraction rate, the trend of heat extraction rate in our study is different from the trend of outlet temperature in Wang et al. (2017).

Figure 2 also suggests that as the rock thermal conductivity values increase, the heat extraction rate also increases in all three rock types. Moreover, there is a more noticeable change of heat extraction rate in scenario #1A–C than in scenario #1D–F and scenario #1G–I. This is because sandstone has a wider range of thermal conductivity value than limestone and granite. By comparing the results of scenario #1A with scenario #1C, we could observe that when the rock thermal conductivity is increased from the minimum value (scenario #1A) to the average value (scenario #1B), the heat extraction rate will be improved by 50.9–51.6%. When the rock thermal conductivity is increased from the average value (scenario #1B) to maximum value (scenario #1C), the heat extraction rate can only be improved by 24.5–25.4%. The heat extraction rate, with a double increase in rock thermal conductivity, will not increase exponentially. Chen et al. (2019) also pointed out that the marginal performance gain from increasing soil thermal conductivity is gradually decreasing.

The influence of inner pipe diameter

Figure 3 presents how the heat extraction rate is changing against different inner pipe diameter under different geological conditions (scenario #2A–I). Figure 3 shows that as the inner pipe diameter increases the heat extraction rate decreases, and the heat extraction rate is linearly related to the inner pipe diameter. It is also clear that as the diameter of the inner pipe decreases, the heat extraction rate change in value is minimal. For example, in scenario #2B, when the inner pipe diameter decreases from 0.10 to 0.05 m, the heat extraction rate increases from 147.7 to 150.4 W m^{-1}, only 1.8% was improved. In addition, the reduction of the inner pipe diameter can be regarded as an increase to

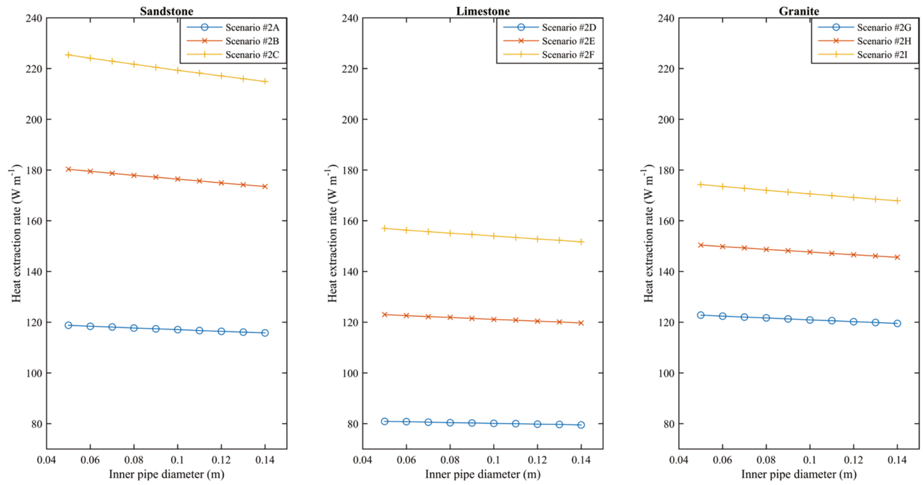

Fig. 3 Influence of different inner pipe diameters on heat extraction rate under different geological conditions

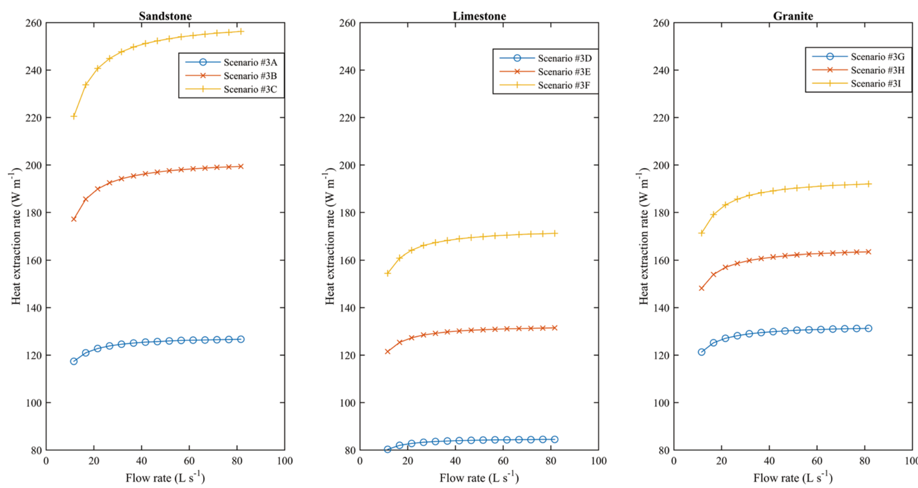

Fig. 4 Influence of different flow rates on heat extraction rate under different geological conditions

the outer pipe diameter, the purpose of which is to increase the area of the annular space and improve the heat transfer capacity.

The influence of flow rate

From scenario #3A–I, we evaluated the influence of flow rate on heat extraction rate under different geological conditions, and the results are depicted in Fig. 4. Figure 4 indicates that as the flow rate increases, the heat extraction rate increases rapidly at first. However, the trend of growth in the heat extraction rate will continue to decrease and eventually terminate. Bu et al. (2012) and Wang et al. (2017) also found that with an increase in flow rate, the heat transfer capacity would continue to increase. This trend is similar to that illustrated in Fig. 4, with an increase that eventually becomes minimal. This implies that increasing only the flow rate may not lead to an increase in the heat extraction rate. Hence, there is an optimal flow rate for DBHE. However, Fig. 4 also shows that the optimal flow rate is not constant, but changes with geological conditions. Thus, when designing a DBHE, we should consider the influence of the heterogeneity of geological materials.

Based on the analysis results of outer pipe diameter, inner pipe diameter, and flow rate, we could conclude that altering only one of the three parameters could lead to an increase in the rate of heat extraction. However, changing only one parameter cannot achieve optimal transfer efficiency; therefore, the three parameters need to allocated simultaneously. The key to achieving the optimal transfer efficiency is to ensure the smooth flow of the circulating water in the DBHE, which means to make sure that the area of the annular space matches the area of the cross-section of the inner pipe. Then, an optimal flow rate that ensures that the DBHE achieves the optimal heat extraction rate is required.

The influence of outer pipe materials

Figure 5 illustrates the impacts of pipe materials on heat extraction rate under different geological conditions (scenario #4A to #4I). It is apparent that the outer pipe wall thermal conductivity value has a limited impact on the heat extraction rate. For example, in scenario #4B, when the outer pipe wall thermal conductivity increases by 590%, the heat extraction rate only be improved by 9%. Moreover, when the outer pipe wall thermal conductivity value is large, keeping an increase in the outer pipe wall thermal conductivity value will not affect the heat transfer performance. Figure 5 also shows that the heat transfer performance of DBHE could be improved by applying a steel outer pipe. Nevertheless, installing the steel outer pipe instead of concrete will increase initial investment, as the DBHE is typically 2–3 km long (Chen et al. 2019). Therefore, it is not economical to apply steel outer pipe to improve the performance of DBHE system.

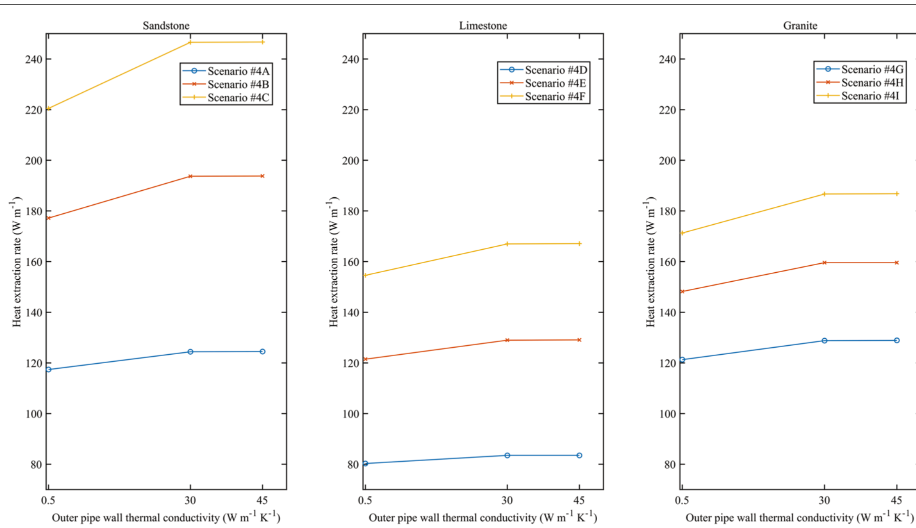

Fig. 5 Influence of outer pipe materials on heat extraction rate under different geological conditions

The influence of grout materials

Figure 6 demonstrates the effects of varying grout thermal conductivity values on heat extraction rate under different geological conditions (scenario #5A to #5I). From Fig. 6, we can see that the optimization effect of applying thermally enhanced grout materials under a good geological condition (high rock thermal conductivity value) is better than that under a poor geological condition (low rock thermal conductivity value). Take scenario #5A and # 5C for example; when we applied thermally enhanced grout material with thermal conductivity value of 1.73 in DBHE under a poor geological condition (scenario #5A), the heat extraction rate will be improved by 4.3%, while in scenario #5C, the heat extraction rate could be increased by 8.2%. In addition, from the results of scenario #5C, we can also observe that when the grout thermal conductivity is increased from 0.73 to 1.73, the heat extraction rate would be improved by 8.2%. When the grout thermal conductivity is increased from 1.73 to 2.77, the heat extraction rate could only be improved by 2.3%. This means the heat extraction rate will not increase exponentially with a double increase in grout thermal conductivity. When compared with the analysis results of pipe materials, it can be concluded that it is more economical to apply thermally enhanced grout materials, instead of using a steel outer pipe.

The influence of DBHE depth

In this study, we defined the depth of 500 m as the lower limit of DBHE in consideration of its heat exchange efficiency. In order to investigate the influence of DBHE depth, the depth range was set from 500 to 3000 m, with an incremental step of 500 m. Figure 7 presents the change in heat extraction rate with DBHE depth under different geological conditions (scenario #6A–I). From Fig. 7, we could find that the heat extraction rate is sensitive to the BHE depth. For instance, in the results of scenario #6B, when we increase the BHE depth from 500 to 1000 m, the heat extraction rate will be increased by approx. 30.0%. However, increasing the DBHE depth will increase the drilling cost. It is, therefore, the optimal design is different for different depth wells.

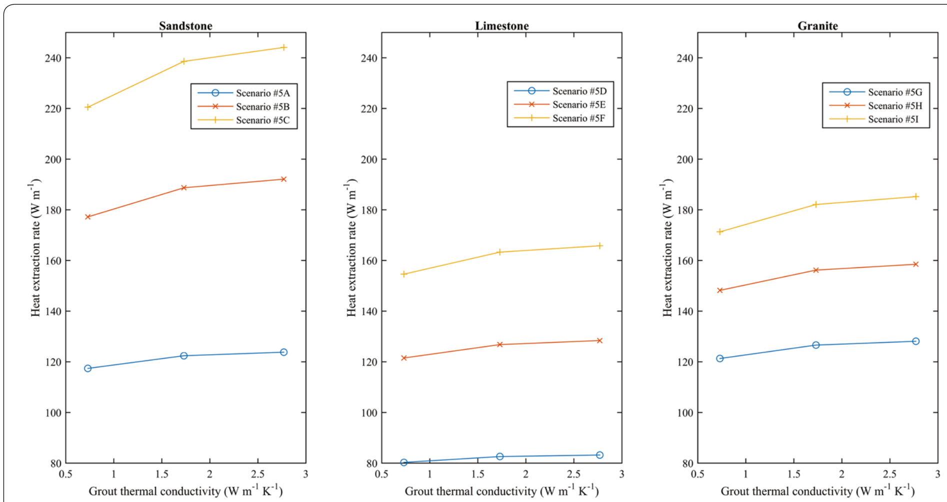

Fig. 6 Influence of grout materials on heat extraction rate under different geological conditions

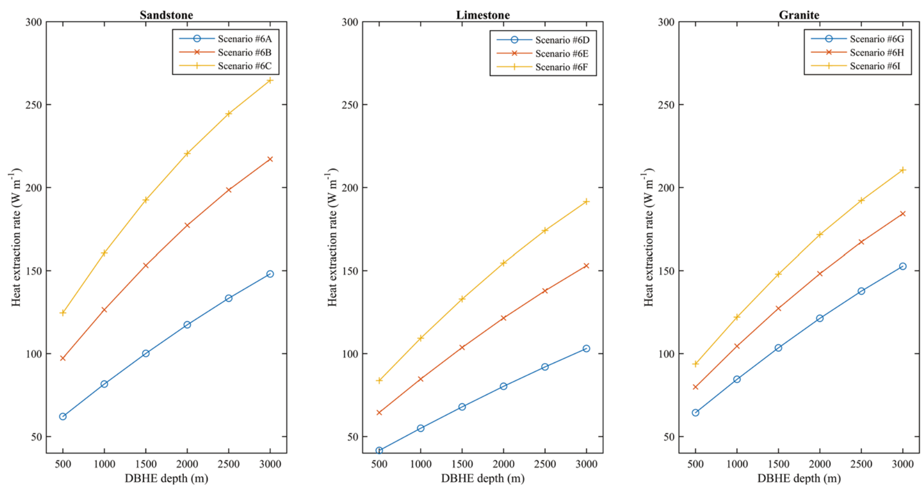

Fig. 7 Influence of DBHE depth on the optimal heat extraction rate under different geological conditions

We should point out that the working time of the system could also affect the heat transfer performance of DBHE. While under continuous heat extraction the difference of outlet temperature after 1 year and after 10 years of operation is minimal (Bu et al. 2012; Kong et al. 2017b; Chen et al. 2019); this phenomenon shows that the mode of continuous heat extraction is not affected by the period of operation. Therefore, the results we simulated are credible, although the long-term analysis is not conducted in this study.

Optimization of DBHE

As mentioned in "Optimization method" section, there is an optimal DBHE design for each depth under certain geological conditions. Therefore, we obtained the optimal DBHE designs for different depths and rock types by applying the index of AEC, as shown in Fig. 8.

Figure 8 shows that the AEC of DBHE in granite and limestone is much higher than the AEC of DBHE in sandstone. Even with a minimum thermal conductivity value, the AEC of DBHE in sandstone is still lower than the AEC of DBHE in granite and limestone because the drilling cost in granite and limestone is much higher than in sandstone. Figure 8 also suggests that the AEC value increases when DBHE depth increases from 500 to 1000 m and deceases when the DBHE depth increases from 1000 to 3000 m. This is because the drilling cost we used was calculated by the relationship between well cost and well depth (Lukawski et al. 2014), and the drilling cost per meter for 1000 m is higher than that for 500 m. When the depth range is 2000–3000 m, the increase of the well depth leads to little increase in drilling cost per meter. Although we employed the relationship between well cost and well depth during the simulation process, there is still a strong uncertainty between the drilling cost and well depth (Lukawski et al. 2014, 2016). In our study, the AEC value decreases when the DBHE depth increases from 1000 to 3000 m, but it does not mean the AEC value will still decrease when the DBHE depth larger than 3000 m. Actually, according to the published well costs, the drilling cost per meter increases rapidly when well depth lager than 3000 m (Gul and Aslanoglu 2018;

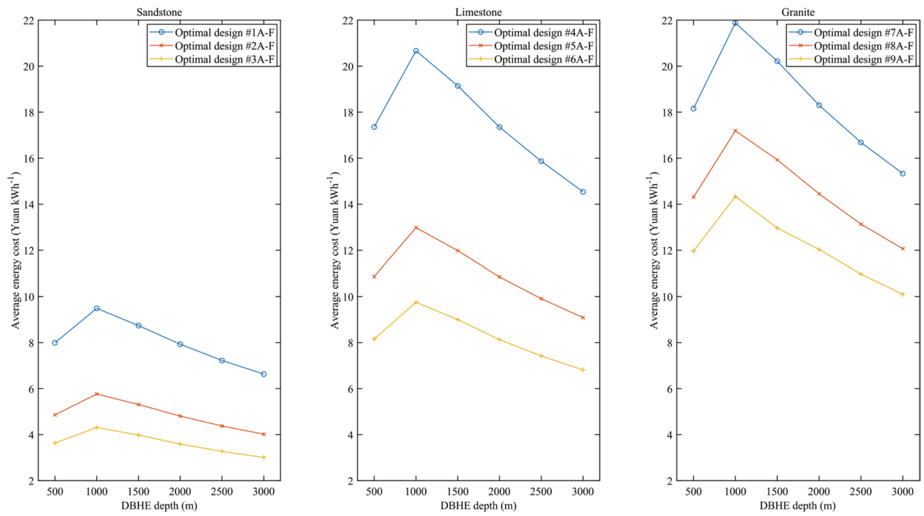

Fig. 8 The average energy cost of DBHE with different depths

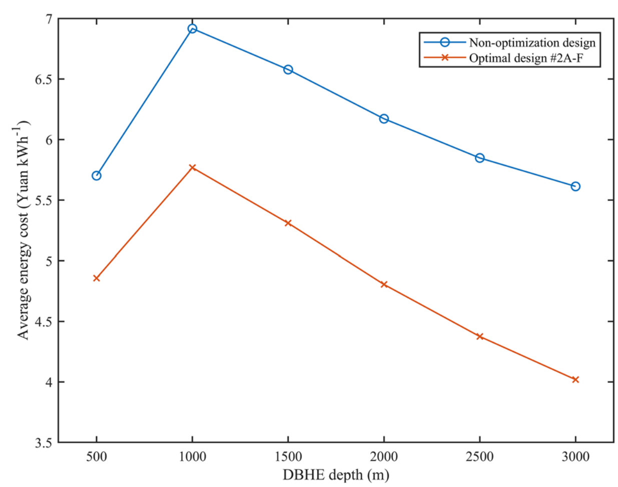

Fig. 9 The comparison of optimal design and non-optimization design

Lukawski et al. 2014, 2016). Therefore, in our cases, a DBHE of 3000 m should be the most economical choice when one wants to get the maximum heat with the lowest cost. In addition, Fig. 8 shows that the AEC value is similar when DBHE depth is 500 and 2000 m, which means the economic benefit of building a 2000 m DBHE is similar to build 4 DBHEs of 500 m. In this case, it is sure one 2000 DBHE is more economical than 4 DBHEs of 500 m due to the lower area demanding.

In order to verify the validity of the optimization method, the non-optimization design was compared to the optimal design under the same geological conditions, as shown in Fig. 9. It is obvious that the optimization method is quite effective. Take the DBHE depth of 500 m as an example, the AEC value decreases 22.1% after optimization. Therefore, the optimization method proposed in this study is robust and can significantly improve the performance of DBHE system.

In our cases, the optimal designs indicate that the most economical outer pipe diameter is 0.220 m because the drilling cost will increase a lot when the outer pipe diameter increases larger than 0.22 m. The most economical outer pipe and grout materials are concrete, and a mix of bentonite and graphite, respectively. The optimal flow rate is different with different well depths and rock types, and the range is 8.5–63 L s^{-1}. Moreover, the steel outer pipe has not been considered in any optimal design, which means it is not economical for DBHE system.

Conclusions and outlook

We carried out a number of sensitivity analyses to identify the effect of design parameters on the heat transfer performance of DBHE. Since the motivation of this work was to obtain the optimal DBHE design, we proposed a procedure to optimize these design parameters. On the basis of these studies, we have drawn the following conclusions.

The heat extraction rate is very sensitive to the outer pipe diameters, well depth, and flow rate. While the grout materials, inner pipe diameter, and outer pipe materials have a minor effect. For fixed rock thermal properties, any increase in the contact area between the circulating water and the rock will enhance the heat extraction rate. Moreover, in order to obtain the optimal design, these parameters need to be allocated simultaneously.

The optimal DBHE designs reveal that the most economical outer and inner pipe diameter was 0.220 m and 0.1544 m, respectively. For fixed pipe diameters, outer pipe materials, grout materials and the optimal flow rate vary with the change of well depths and rock thermal properties. The results also show that it is more economical to apply thermally enhanced grout materials, instead of using a steel outer pipe.

Finally, it should be noted that the heat transfer characteristics of DBHE are also related to several other parameters such as the thermal conductivity of the heat transfer medium, the thermal insulation performance of the inner pipe. Nonetheless, the proposed optimization method can significantly improve the heat transfer performance of DBHE.

List of symbols

Variables

d: Diameter, m; *f*: Friction factor; *c*: Volumetric heat capacity, J m^{-3} K^{-1}; *h*: Convective film coefficient, W m^{-2} K^{-1}; *H*: Ratio of volumetric heat capacities; *k*: Thermal conductivity, W m^{-1} K^{-1}; *A*: Area, m^2; *N*: Dimensionless thermal conductance; *r*: Radius, m; *R*: Thermal resistance, K m W^{-1}; Re: Reynolds number; *T*: Temperature, °C; *V*: Flow velocity, m s^{-1}; *t*: Time, s; *w*: Flow rate, m^3 s^{-1}; z: Vertical depth coordinate, m; Pr: Prandtl number; *P*: Heat extraction rate, W m^{-1}; *Q*: Thermal energy output, J; *C*: Cost, Yuan; *D*: Borehole depth, m.

Greeks

κ: Ratio of thermal conductivities; μ: Viscosity, kg m^{-1} s^{-1}; ρ: Density, kg m^{-3}.

Subscripts

b: Borehole; pi: Inside of inner pipe; po: Outside of inner pipe; pp: Inner pipe; *D*: Dimensionless; eo: Outside of outer pipe; ei: Inside of outer pipe; ep: Outer pipe; *f*: Circulating fluid; *g*: Grout; *s*: Ground (or soil); 1: Flow path number 1; 2: Flow path number 2.

Acknowledgements

This research is supported by the National Key Research and Development Program of China (No. 2018YFB1501801).

Authors' contributions

SP performed the simulations. SP and YK prepared the manuscript. CC provided the Matlab code. YK, CC, ZP and JW improved and revised the manuscript. All authors read and approved the final manuscript.

Availability of data and materials
The datasets generated and analyzed during the current study are available from the corresponding author on reasonable request.

Consent for publication
Not applicable.

Competing interests
The authors declare that they have no competing interests.

Author details
[1] Key Laboratory of Shale Gas and Geoengineering, Institute of Geology and Geophysics, Chinese Academy of Sciences, Beijing 100029, China. [2] Innovation Academy for Earth Science, Chinese Academy of Sciences, Beijing 100029, China. [3] University of Chinese Academy of Sciences, Beijing 100049, China. [4] Helmholtz Centre for Environmental Research-UFZ, 04318 Leipzig, Germany.

Received: 26 September 2019 Accepted: 27 January 2020
Published online: 05 February 2020

References

Acuña J, Mogensen P, Palm B. Distributed thermal response tests on a multi-pipe coaxial borehole heat exchanger. HVAC & R Res. 2011;17(6):1012–29.
Acuña J, Palm B. Distributed thermal response tests on pipe-in-pipe borehole heat exchangers. Appl Energy. 2013;109:312–20.
Alimonti C, Soldo E. Study of geothermal power generation from a very deep oil well with a wellbore heat exchanger. Renew Energy. 2016;86:292–301.
Alimonti C, Soldo E, Bocchetti D, Berardi D. The wellbore heat exchangers: a technical review. Renew Energy. 2018;123:353–81.
Beier RA, Acuña J, Mogensen P, Palm B. Borehole resistance and vertical temperature profiles in coaxial borehole heat exchangers. Appl Energy. 2013;102:665–75.
Beier RA. Transient heat transfer in a U-tube borehole heat exchanger. Appl Therm Eng. 2014;62(1):256–66.
Beier RA, Acuña J, Mogensen P, Palm B. Transient heat transfer in a coaxial borehole heat exchanger. Geothermics. 2014;51:470–82.
Beier RA, Holloway WA. Changes in the thermal performance of horizontal boreholes with time. Appl Therm Eng. 2015;78:1–8.
Bu X, Ma W, Li H. Geothermal energy production utilizing abandoned oil and gas wells. Renew Energy. 2012;41:80–5.
Cho WJ, Kwon S, Choi JW. The thermal conductivity for granite with various water contents. Eng Geol. 2009;107(3–4):167–71.
Clauser C. Thermal storage and transport properties of rocks, I: heat capacity and latent heat. Encycl Solid Earth Geophys. 2011a;2:1423–31.
Clauser C. Thermal storage and transport properties of rocks, II: thermal conductivity and diffusivity. Encycl Solid Earth Geophys. 2011b;2:1431–48.
Cheng W, Li T, Nian Y, Wang C. Studies on geothermal power generation using abandoned oil wells. Energy. 2013;59:248–54.
Chen C, Shao H, Naumov D, Kong Y, Tu K, Kolditz O. Numerical investigation on the performance, sustainability, and efficiency of the deep borehole heat exchanger system for building heating. Geotherm Energy. 2019;7(1):18.
Daniilidis A, Alpsoy B, Herber R. Impact of technical and economic uncertainties on the economic performance of a deep geothermal heat system. Renew Energy. 2017;114:805–16.
Fang L, Diao N, Shao Z, Zhu K, Fang Z. A computationally efficient numerical model for heat transfer simulation of deep borehole heat exchangers. Energy Build. 2018;167:79–88.
Gul S, Aslanoglu V. Drilling and well completion cost analysis of geothermal wells in Turkey. SGP–TR–213. In: Proceedings of 43rd Workshop on Geothermal Reservoir Engineering Stanford University, Stanford, California, 12–14, February, 2018.
Heidinger P. Integral modeling and financial impact of the geothermal situation and power plant at Soultz-sous-Forêts. CR Geosci. 2010;342(7–8):626–35.
Holmberg H, Acuña J, Næss E, Sønju O. Thermal evaluation of coaxial deep borehole heat exchangers. Renew Energy. 2016;97:65–76.
Kohl T, Brenni R, Eugster W. System performance of a deep borehole heat exchanger. Geothermics. 2002;31:687–708.
Kong Y, Pang Z, Shao H, Hu S, Kolditz O. Recent studies on hydrothermal systems in China: a review. Geotherm Energy. 2014;2:19.
Kong Y, Pang Z, Shao H, Kolditz O. Optimization of well-doublet placement in geothermal reservoirs using numerical simulation and economic analysis. Environ Earth Sci. 2017a;76:118. https://doi.org/10.1007/s12665-017-6404-4.
Kong Y, Chen C, Pang Z, Shao H, Xiong L, Wang J. Principle and capacity quantification of deep-borehole heat exchangers. Chin J Geophys. 2017b;60(12):4741–52.
Kujawa T, Nowak W, Stachel A. Utilization of existing deep geological wells for acquisitions of geothermal energy. In: Thermal Sciences 2004. Proceedings of the ASME-ZSIS International Thermal Science Seminar II. Begel House Inc.; 2004.
Lhendup T, Aye L, Fuller RJ. In-situ measurement of borehole thermal properties in Melbourne. Appl Therm Eng. 2014;73(1):287–95.

Le Lous M, Larroque F, Dupuy A, Moignard A. Thermal performance of a deep borehole heat exchanger: insights from a synthetic coupled heat and flow model. Geothermics. 2015;57:157–72.
Liu X, Polsky Y, Qian D, Mcdonald J. Analysis of cost reduction potential of vertical bore ground heat exchanger (Final). Oak Ridge: Oak Ridge National Lab; 2018.
Lukawski MZ, Anderson BJ, Augustine C, Capuano LE, Beckers KF, Livesay B, Tester JW. Cost analysis of oil, gas, and geothermal well drilling. J Pet Sci Eng. 2014;118:1–14.
Lukawski MZ, Silverman RL, Tester JW. Uncertainty analysis of geothermal well drilling and completion costs. Geothermics. 2016;64:382–91.
Luo Y, Guo H, Meggers F, Zhang L. Deep coaxial borehole heat exchanger: Analytical modeling and thermal analysis. Energy. 2019;185:1298–313.
McKenna TE, Sharp Jr JM, Lynch FL. Thermal conductivity of Wilcox and Frio sandstones in south Texas (Gulf of Mexico Basin). AAPG Bull. 1996;80(8):1203–15.
Nalla G, Shook G, Mines G, Bloomfield K. Parametric sensitivity study of operating and design variables in wellbore heat exchangers. Geothermics. 2005;34(3):330–46.
Noorollahi Y, Pourarshad M, Jalilinasrabady S, Yousefi H. Numerical simulation of power production from abandoned oil wells in Ahwaz oil field in southern Iran. Geothermics. 2015;55:16–23.
Olasolo P, Juárez MC, Olasolo J, Morales MP, Valdani D. Economic analysis of Enhanced Geothermal Systems (EGS). A review of software packages for estimating and simulating costs. Appl Therm Eng. 2016;104:647–58.
Rybach L, Hopkirk R. Shallow and deep borehole heat exchangers—achievements and prospects. World Geotherm Congress. 1995;1995:2133–9.
Rybach L. Geothermal energy: sustainability. Geothermics. 2003;32(4–6):463–70.
Raymond J, Mercier S, Nguyen L. Designing coaxial ground heat exchangers with a thermally enhanced outer pipe. Geotherm Energy. 2015;3(1):7.
Rodríguez R, Díaz MB. Analysis of the utilization of mine galleries as geothermal heat exchangers by means a semi-empirical prediction method. Renew Energy. 2009;34(7):1716–25.
Sapinskasliwa A, Rosen MA, Gonet A, Sliwa T. Deep borehole heat exchangers—a conceptual and comparative review. Int J Air-Condition Refrig. 2016;24(01):1630001.
Su Y, Yang F, Wang B, Jia Z, Duan Z. Reinjection of cooled water into sandstone geothermal reservoirs in China: a review. Geosci J. 2018;22(1):199–207.
Templeton J, Ghoreishi-Madiseh S, Hassani F, Al-Khawaja M. Abandoned petroleum wells as sustainable sources of geothermal. Energy. 2014;70:366–73.
Thomas Jr J, Frost RR, Harvey RD. Thermal conductivity of carbonate rocks. Eng Geol. 1973;7(1):3–12.
Ungemach P. Reinjection of cooled geothermal brines into sandstone reservoirs. Geothermics. 2003;32(4):743–61.
Wang J. Geothermics and its applications. Beijing: Science Press; 2015.
Wang Z, Wang F, Liu J, Ma Z, Han E, Song M. Field test and numerical investigation on the heat transfer characteristics and optimal design of the heat exchangers of a deep borehole ground source heat pump system. Energy Convers Manage. 2017;153:603–15.
Wight N, Bennett N. Geothermal energy from abandoned oil and gas wells using water in combination with a closed wellbore. Appl Therm Eng. 2015;89:908–15.
Zanchini E, Lazzari S, Priarone A. Improving the thermal performance of coaxial borehole heat exchangers. Energy. 2010;35(2):657–66.

Publisher's Note

Springer Nature remains neutral with regard to jurisdictional claims in published maps and institutional affiliations.